Available online at http://scik.org
Commun. Math. Biol. Neurosci. 2020, 2020:10
https://doi.org/10.28919/cmbn/4315
ISSN: 2052-2541

OPTIMAL CONTROL PROBLEM OF A QUARANTINE MODEL IN MULTI REGION WITH SPATIAL DYNAMICS

SOUKAINA BEN RHILA*, RACHID GHAZZALI, AMINE EL BHIH, MOSTAFA RACHIK

Laboratory of Analysis Modeling and Simulation, Department of Mathematics and Computer Science, Faculty of Sciences Ben M'Sik, Hassan II University Casablanca, BP 7955, Sidi Othman, Casablanca, Morocco

Abstract. Firstly we define a multi-region discrete SIR model describing the spread of an epidemic that can emerge in one region and spread to regions that are connected to its neighbors by any type of anthropological movement. We assume that the infected who leave the main source of epidemic or other areas that were partially affected later, in order to enter safer areas, represent the population category to be controlled, and we consider a surface colored cell grid is presented to illustrate the entire domain affected by the epidemic, each cell may represent a subdomain or region. Secondly we introduce a control variable into our model to show the effectiveness of movement restrictions of infected individuals from the primary source we target by a quarantine optimal control strategy. The characterization of the sought optimal control is derived from Pontryagin's Maximum Principle. Numerical illustrations are given to the obtained results.

Keywords: multi-region; spatial SIR model; quarantine; optimal control.

2010 AMS Subject Classification: 93A30.

1. INTRODUCTION

Nowadays, it is no longer necessary to justify the importance of spatial dynamics in the description and analysis of infectious diseases. Indeed, the spatio-temporal spread of epidemic

*Corresponding author
E-mail address: benrhila.soukaina@gmail.com
Received September 24, 2019

diseases was noticed very early, the case of SARS epidemic of spring 2003 clearly showed that human diseases spread in space, over large areas and often jumping continents [1]. These cases also includes the influenza pandemic (H1N1) 2009 [2], first appeared in Mexico and then spread rapidly throughout the world, the Black Death that appeared in the 1300s in Europe [3], followed by Measles and smallpox in the New World between the 1500s and 1600s [4], [5] More recently, Ebola appeared in the Democratic Republic of the Congo in 1977, in Sudan in 1979 and in North America in the late 1990s [6, 7] and HIV / AIDS appeared in 1981 [8].

Relatively few that are focused on the spatio-temporal model, a related and important concept in epidemiological mathematical models. In most mathematical models, the existence of a spatial component has a remarkable probability due to the movements of thousands of people moving from one region to another, in this case an epidemic can spread rapidly around a vast area given regardless of the border. The geographic scale is therefore at the heart of a multitude of studies of diseases that are becoming spatially mobile to different regions because of the movement of people from one region to another.

Control of epidemics is becoming increasingly important for governments and public health officials. More specifically, it seeks to understand the spatial dynamics of the spread of infectious diseases in order to develop prevention and intervention strategies aimed at reducing their impact on public health. It is hoped that the interplay of spatial factors in the mathematical models of infectious diseases will help us better understand, predict and ultimately control the behavior of this phenomenon. One of the most basic strategies for controlling the spread of infectious diseases is quarantine through travel restrictions by blocking free travelers, traders and carriers, or stopping interactions with others. taking the example of EVD epidemics in several countries in sub-saharan Africa [9, 10, 11]. Before the detection of the disease, the mega-flow of infected people leaving one city to another is considered important, before the political policy in Guinea prohibits all population movements going to Liberia in order to limit the spread of the virus, particularly after the diagnosis of some infected cases in Liberia in March 2014 [12].

After studying several papers taking into account the spatial aspect of the spread of an epidemic [13, 14, 15]. We study the behavior and effect of quarantine in a SIR discrete-time multi-region model for all epidemics that are likely to spread rapidly in many places. For this, it

is assumed here that the epidemic can be transmitted and spread from a region to its neighborhood by the movement of infected people leaving the main source of epidemic or other areas that were partially affected later, in order to penetrate into safer areas. Any kind of diseases that respects this rule, can be modelled and controlled with our approach. We consider a control goal that aims to reduce the spread of the epidemic by introducing a quarantine control variable into the multi-region discrete SIR model corresponding to the primary source of infection to control. These controls restrict the movement of infected individuals from the target area to limit contact between susceptible people and infected people.

The rest of the manuscript is organized as follows: In Section 2, we describe the mathematical model. The objective is the functional analysis and the analysis of the controlled approach to the field of cell control, are given in Section 3 with the introduction of numerical simulations. Finally, we conclude our work in Section 4.

2. MATHEMATICAL MODEL SIR

We consider a discrete-time SIR model modelling the spread of an epidemic within a domain Ω , occuped by an homogeneous population, that is divided to M^2 cells uniforme in size $\Omega = \bigcup_{p,q=1,..,M} C_{pq}$ and let $N_i^{C_{pq}}$ be the population of C_{pq} at time i , i.e., the number of individuals in C_{pq}, where C_{pq} denoting spatial location of infection.

According to the disease transmission mechanism, a host can be Susceptible, Infective, or Recovered. Susceptible individuals are those who are healthy and do not carry the epidemic but can contract it from infective hosts. Infective hosts carry the contagion and are able to pass it on to another host. Finally, recovered hosts are those who are no longer infective and have acquired immunity from future infection. Note that this immunity is not necessarily everlasting and that the transition between the $S_i^{C_{pq}}$, $I_i^{C_{pq}}$ and $R_i^{C_{pq}}$ states is probabilistic, with probabilities being determined by the observed characteristics of specific diseases.

In addition to the death , there are population movements among those three epidemiological compartments ,from time unit i to time $i+1$. The unit of time i can correspond to days, months or years, it depends on the frequency of data collection and statistics. The relation between the regions C_{pq} and C_{rs} is defined as follows: We say that $C_{pq} = \bigcap V_{rs}, \forall (r,s) \in \{1...M\}^2$ means

that $C_{rs} \in V_{pq}$, where V_{pq} the Vicinity set or Neighborhood of a cell C_{pq} and we define the Vicinity set of C_{pq} ;

V_{pq}=$\left\{C_{rs} \in \Omega / r = p+k, s = q+k', (k,k') \in \{-1,0,1\}^2\right\}$. We assume that the susceptible individuals not yet infected but can be infected only through contacts with infectives of a source C_{pq}, thus, the infection transmission is assumed to occur between individuals present in a given cell C_{rs} and is given by

$$\sum_{C_{rs} \in V_{pq}} \beta_{rs} I_i^{C_{pq}} S_i^{C_{rs}}$$

where the disease transmission coefficient $\beta_{rs} > 0$, is the proportion of contacts between an infective from a cell C_{pq} and a susceptible from its neighbor cell $C_{rs} \in V_{pq}$.

The following system describes the multi-regions discrete SIR model corresponding to cell C_{pq},

for $p,q = 1,\ldots,M$, we have

$$\begin{aligned} S_{i+1}^{C_{pq}} &= \Lambda^{C_{pq}} + S_i^{C_{pq}} - \beta_{pq} I_i^{C_{pq}} S_i^{C_{pq}} - \sum_{C_{rs} \in V_{pq}} \beta_{rs} I_i^{C_{pq}} S_i^{C_{rs}} \\ &\quad - d^{C_{pq}} S_i^{C_{pq}} \qquad (1) \end{aligned}$$

$$\begin{aligned} I_{i+1}^{C_{pq}} &= I_i^{C_{pq}} + \beta_{pq} I_i^{C_{pq}} S_i^{C_{pq}} + \sum_{C_{rs} \in V_{pq}} \beta_{rs} I_i^{C_{pq}} S_i^{C_{rs}} \\ &\quad - \left(\alpha^{C_{pq}} + \gamma^{C_{pq}} + d^{C_{pq}}\right) I_i^{C_{pq}} \qquad (2) \end{aligned}$$

$$R_{i+1}^{C_{pq}} = R_i^{C_{pq}} + \gamma^{C_{pq}} I_i^{C_{pq}} - d^{C_{pq}} R_i^{C_{pq}} \qquad (3)$$

where $S_0^{C_{pq}}$, $I_0^{C_{pq}}$ and $R_0^{C_{pq}}$ are the given initial state in the region C_{pq}. In equations (1)-(3), all parameters are non-negative. Following the contacts between a susceptible and an infective from the cell C_{pq} with β_{pq} rate, $d^{C_{pq}} > 0$ is the natural death rate, $\alpha^{C_{pq}} > 0$ is death rate due to the infection, $\gamma^{C_{pq}} > 0$ denote the recovery rate of infectives and $\Lambda^{C_{pq}}$ birth rate in C_{pq}. By assuming that is occupied by an homogeneous population, $\alpha^{C_{pq}}, d^{C_{pq}}$ and $\gamma^{C_{pq}}$ are assumed to be the same for all cells of Ω .

the population size corresponding to cell C_{pq} at time i. It is clear that the population size remains constant if $d^{C_{pq}} = \frac{\Lambda^{C_{pq}}}{N_i^{C_{pq}}}$, in fact

$$\begin{aligned} N_{i+1}^{C_{pq}} &= S_{i+1}^{C_{pq}} + I_{i+1}^{C_{pq}} + R_{i+1}^{C_{pq}} \\ &= S_i^{C_{pq}} + I_i^{C_{pq}} + R_i^{C_{pq}} + \Lambda^{C_{pq}} - d^{C_{pq}} \left(S_i^{C_{pq}} + I_i^{C_{pq}} + R_i^{C_{pq}} \right) \\ &= N_i^{C_{pq}} + \Lambda^{C_{pq}} - d^{C_{pq}} N_i^{C_{pq}} = N_i^{C_{pq}}. \end{aligned}$$

In this case, Fig.1(a), Fig.1(b) and Fig.1(c) describe the dynamics of susceptible, infected populations and removed in the case where no control strategy is yet suggested (see the differential system (1) - (3)) and we note that in all these figures presented here, simulations give us an idea of the propagation of the epidemic in the case where the infection begins in the three C_{11}, C_{55} and C_{1010} regions characterized by different parameters listed in Table 1.

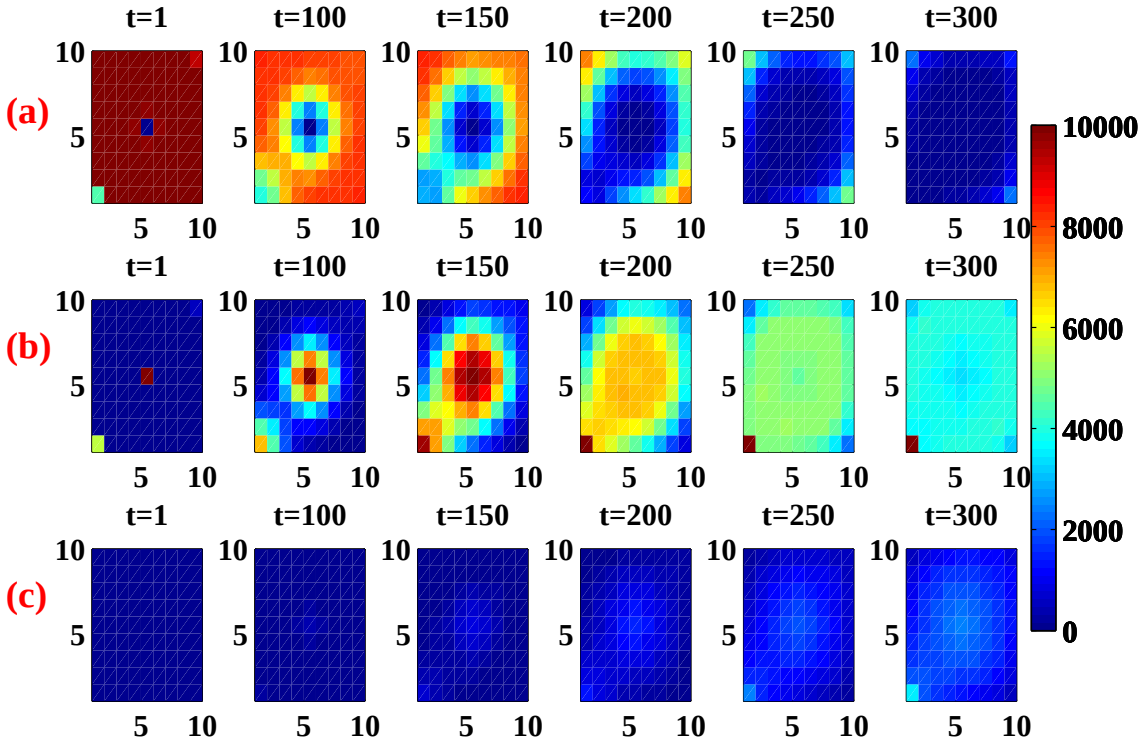

FIGURE 1. States of system (1)–(3) without controls. (a) Susceptibles behavior in the absence of control. (b) Infectives behavior in the absence of control. (c) Removed behavior in the absence of control

It observed in Fig.1(a) a uniform wave front propagating the disease from each source of infection, after 200 days we can see that in most cells, $S^{C_{pq}}$ becomes less important, taking values between 0 and 2000 in regions close to each source of infection, while in others regions (cells), it takes values between 4000 and 7000 except $S^{C_{10,1}}$ and $S^{C_{1,10}}$, they keep their values in 10.000 since it is located far from the sources of the infection.

In Fig.1(b) we can further observe the spatial spread of infection in regions or cells of Ω, when we consider a nonzero initial infection condition in cell $C_{10,10}$, located in the upper right corner , C_{11} the lower left corner and C_{55} in the middle, the number of infected people increases rapidly. after 200 days we see that $I^{C_{pq}}$ takes values between 4000 and 7000 except at the two opposite corners of the infection and at some cells at the borders where there is no infected person yet. Finally, at later times, $I^{C_{pq}}$ converges to 5000 in most cells at $i = 250$ and in all cells at $i = 300$, because as we move forward in time, some people acquire immune responses that help to naturally cure the disease. As we can clearly deduce in Fig.1(c), that after 200 days the number $R^{C_{pq}}$ is not zero and takes values between 500 and 1000, except for the distant cells where it remains zero. Finally, at later times, $R^{C_{pq}}$ converges to 1000 in most cells at $i = 250$ and in all cells at $i = 300$, because as we progress in time, some people acquire immune responses that help them to heal naturally of the disease.

3. AN OPTIMAL CONTROL PROBLEM

Optimal control approach has been applied to models(1)-(3) to reduce the number of infected from leaving the regions C_{pq}, in order to arrest all movements from domains region source C_{pq} controlled, to the vicinity C_{rs}, along the control strategy period. For this we introduce a control variable $u_i^{C_{rs}}$ $(C_{rs} \in V_{pq})$ which represents the quarantine.

To show the effectiveness rate of the quarantine approach, the mathematical model with control is described based on the following differential system.

$$
\begin{aligned}
S_{i+1}^{C_{pq}} &= \Lambda^{C_{pq}} + S_i^{C_{pq}} - \beta_{pq} I_i^{C_{pq}} S_i^{C_{pq}} - \sum_{C_{rs} \in V_{pq}} u_i^{rsC_{pq}} \beta_{rs} I_i^{C_{pq}} S_i^{C_{rs}} \\
&\quad - d^{C_{pq}} S_i^{C_{pq}} \qquad (4) \\
I_{i+1}^{C_{pq}} &= I_i^{C_{pq}} + \beta_{pq} I_i^{C_{pq}} S_i^{C_{pq}} + \sum_{C_{rs} \in V_{pq}} u_i^{pqC_{rs}} \beta_{rs} I_i^{C_{rs}} S_i^{C_{pq}} \\
&\quad - \left(\alpha^{C_{pq}} + \gamma^{C_{pq}} + d^{C_{pq}} \right) I_i^{C_{pq}} \qquad (5) \\
R_{i+1}^{C_{pq}} &= R_i^{C_{pq}} + \gamma^{C_{pq}} I_i^{C_{pq}} - d^{C_{pq}} R_i^{C_{pq}} \qquad (6)
\end{aligned}
$$

We are interested in controlling the population of cells C_{pq}. Then, the problem is to minimize the objective functional given by

$$
J(u_i^{pqC_{rs}}) = \psi_1 I_N^{C_{pq}} - \psi_2 R_N^{C_{pq}} + \sum_{C_{rs} \in V_{pq}} \sum_{i=1}^{N-1} \left(\psi_1 I_i^{C_{pq}} - \psi_2 R_i^{C_{pq}} + \frac{A_{rs}}{2} (u_i^{pqC_{rs}})^2 \right)
$$

subject to system (4)-(6), Here ψ_1 and ψ_2 are positive constants to keep a balance in the size of $I_i^{C_{pq}}$ and $R_i^{C_{pq}}$ respectively. In the objective functional, A_{rs} is the positive weight parameters which are associated with the control $u_i^{pqC_{rs}}$.

Our goal is to minimize the infectives, while minimizing the cost of the quarantine control strategy in the cell C_{pq} . In other words, we are seeking an optimal control $u_i^{pqC_{rs}{}^*}$ such that

$$
J(u_i^{pqC_{rs}{}^*}) = \min\{J(u) \mid (u) \in \mathscr{U}_{ad}\}, \qquad (7)
$$

where $\mathscr{U}_{ad}$ is the set of admissible controls defined by

$$
\mathscr{U}_{ad} = \{(u) \, | u^{min} \leq u_i \leq u^{max}, \, i \in \{0 \ldots, N-1\} \},
$$

where $(u^{min}, u^{max}) \in]0,1[^2$.

The sufficient condition for existence of an optimal control for the problem follows from the following theorem

Theorem 3.1. *(Sufficient conditions)*

For the optimal control problem given by (7) along with the state equations (4)-(6), there exists a control $(u_i^{pqC_{rs}*}) \in \mathscr{U}_{ad}$ *such that*

$$J(u_i^{pqC_{rs}*}) = min\{J(u)/(u) \in \mathscr{U}_{ad}\}$$

Proof. See Dabbs, K [16], Theorem 1. □

At the same time by using Pontryagin's Maximum Principle [17] we derive necessary conditions for our optimal control. For this purpose we define the Hamiltonian as:

$$\begin{aligned}
\mathscr{H}(\Omega) &= \sum_{C_{rs} \in V_{pq}} \left(\psi_1 I_i^{C_{pq}} - \psi_2 R_i^{C_{pq}} + \frac{A_{rs}}{2} (u_i^{pqC_{rs}})^2 \right) \\
&+ \sum_{p,q=1}^{M} \zeta_{1,i+1} \left(\Lambda^{C_{pq}} + S_i^{C_{pq}} - \beta_{pq} I_i^{C_{pq}} S_i^{C_{pq}} - \sum_{C_{rs} \in V_{pq}} u_i^{rsC_{pq}} \beta_{rs} I_i^{C_{pq}} S_i^{C_{rs}} - d^{C_{pq}} S_i^{C_{pq}} \right) \\
&+ \zeta_{2,i+1} \left(I_i^{C_{pq}} + \beta_{pq} I_i^{C_{pq}} S_i^{C_{pq}} + \sum_{C_{rs} \in V_{pq}} u_i^{pqC_{rs}} \beta_{rs} I_i^{C_{pq}} S_i^{C_{rs}} - \left(\alpha^{C_{pq}} + \gamma^{C_{pq}} + d^{C_{pq}} \right) I_i^{C_{pq}} \right) \\
&+ \zeta_{3,i+1} \left[R_i^{C_{pq}} + \gamma^{C_{pq}} I_i^{C_{pq}} - d^{C_{pq}} R_i^{C_{pq}} \right] \Big)
\end{aligned}$$

Theorem 3.2. *(Necessary Conditions)*

Given an optimal control $(u_i^{pqC_{rs}*})$ *and solutions* $S_i^{C_{pq}*}, I_i^{C_{pq}*}$ *and* $R_i^{C_{pq}*}$,

there exists $\zeta_{k,i}$, $i = 1...N$, $k = 1,2,3$, *the adjoint variables satisfying the following equations:*

$$\begin{aligned}
\zeta_{1,i} &= \left(2 - d^{C_{pq}}\right) \zeta_{1,i+1} + \left(\beta_{pq} I_i^{C_{pq}} + \sum_{C_{rs} \in V_{pq}} u_i^{rsC_{pq}} \beta_{rs} I_i^{C_{pq}} \right) (\zeta_{2,i+1} - \zeta_{1,i+1}) \\
\zeta_{2,i} &= \psi_1 + \beta_{pq} S_i^{C_{pq}} (\zeta_{2,i+1} - \zeta_{1,i+1}) + \left(2 - \left(\alpha^{C_{pq}} + d^{C_{pq}}\right)\right) \zeta_{2,i+1} + \gamma^{C_{pq}} (\zeta_{3,i+1} - \zeta_{2,i+1}) \\
\zeta_{3,i} &= -\psi_2 + \left(2 - d^{C_{pq}}\right) \zeta_{3,i+1}
\end{aligned}$$

$\zeta_{2,N} = \psi_1$ *and* $\zeta_{3,N} = \psi_2$.

Furthermore, the optimal control $(u_i^{pqC_{rs}*})$ *is given by*

$$u_i^{pqC_{rs}*} = min\{max\{u^{min}, \frac{(\zeta_{1,i+1}-\zeta_{2,i+1})\beta_{rs}I_i^{C_{pq}}S_i^{C_{rs}}}{A_{rs}}\}, u^{max}\}\}, \;\; i=1,...,n.$$

Proof. Using Pontryagin's Maximum Principle [17] and setting $S_i^{C_{rs}} = S_i^{C_{rs}*}$, $I_i^{C_{rs}} = I_i^{C_{rs}*}$, $R_i^{C_{rs}} = R_i^{C_{rs}*}$ and $u_i^{pqC_{rs}} = u_i^{pqC_{rs}}$. we obtain the following adjoint equations:

$$\begin{aligned}
\Delta\zeta_{1,i} &= -\frac{\partial\mathscr{H}}{\partial S_i^{C_{pq}}} = -\left[\left(1-d^{C_{pq}}\right)\zeta_{1,i+1} + \left(\beta_{pq}I_i^{C_{pq}} + \sum_{C_{rs}\in V_{pq}} u_i^{rsC_{pq}}\beta_{rs}I_i^{C_{pq}}\right)(\zeta_{2,i+1}-\zeta_{1,i+1})\right] \\
\Delta\zeta_{2,i} &= -\frac{\partial\mathscr{H}}{\partial I_i^{C_{pq}}} = -\left[\psi_1 + \beta_{pq}S_i^{C_{pq}}(\zeta_{2,i+1}-\zeta_{1,i+1}) + \left(1-\left(\alpha^{C_{pq}}+d^{C_{pq}}\right)\right)\zeta_{2,i+1} + \gamma^{C_{pq}}(\zeta_{3,i+1}-\zeta_{2,i+1})\right] \\
\Delta\zeta_{3,i} &= -\frac{\partial\mathscr{H}}{\partial R_i^{C_{pq}}} = -\left[-\psi_2 + \left(1-d^{C_{pq}}\right)\zeta_{3,i+1}.\right]
\end{aligned} \tag{3.8}$$

then

$$\zeta_{1,i} = \left(2-d^{C_{pq}}\right)\zeta_{1,i+1} + \left(\beta_{pq}I_i^{C_{pq}} + \sum_{C_{rs}\in V_{pq}} u_i^{rsC_{pq}}\beta_{rs}I_i^{C_{pq}}\right)(\zeta_{2,i+1}-\zeta_{1,i+1})$$

$$\zeta_{2,i} = \psi_1 + \beta_{pq}S_i^{C_{pq}}(\zeta_{2,i+1}-\zeta_{1,i+1}) + \left(2-\left(\alpha^{C_{pq}}+d^{C_{pq}}\right)\right)\zeta_{2,i+1} + \gamma^{C_{pq}}(\zeta_{3,i+1}-\zeta_{2,i+1})$$

$$\zeta_{3,i} = -\psi_2 + \left(2-d^{C_{pq}}\right)\zeta_{3,i+1}$$

To obtain the optimality conditions we take the variation with respect to control $u_i^{pqC_{rs}}$ and set it equal to zero

$$\frac{\partial\mathscr{H}}{\partial u_i^{pqC_{rs}}} = A_{rs}u_i^{pqC_{rs}} - \zeta_{1,i+1}\sum_{C_{rs}\in V_{pq}}\beta_{rs}I_i^{C_{pq}}S_i^{C_{rs}} + \zeta_{2,i+1}\sum_{C_{rs}\in V_{pq}}\beta_{rs}I_i^{C_{pq}}S_i^{C_{rs}} = 0$$

Then we obtain the optimal controls

$$u_i^{pqC_{rs}} = \frac{(\zeta_{1,i+1}-\zeta_{2,i+1})\beta_{rs}I_i^{C_{pq}}S_i^{C_{rs}}}{A_{rs}}, \;\; i=1,...,n \;\; / \;\; C_{rs}\in V_{pq}$$

By the bounds in $\mathscr{U}_{ad}$ of the control, it is easy to obtain $u_i^{pqC_{rs}*}$ in the following form

$$u_i^{pqC_{rs}*} = min\{max\{u^{min}, \frac{(\zeta_{1,i+1}-\zeta_{2,i+1})\beta_{rs}I_i^{C_{pq}}S_i^{C_{rs}}}{A_{rs}}\}, u^{max}\}, \;\; i=1,...,n \;\; / \;\; C_{pq}\in V_{rs}$$

□

3.1. Numerical simulation. We now present numerical simulations associated with the above mentioned optimal control problem. We wrote a code in MATLAB^{TM} and simulated our results using different data. We solve the optimality system using an iterative method. Where the state system with an initial guess is solved forward in time and then the adjoint system is solved backward in time because of the transversality conditions. Afterwards, we updated the optimal controls values using the values of state and costate variables obtained in the previous steps. Finally, we execute the previous step still a tolerance criterion is reached.

In order to show the importance of our work and without lose of generality, we consider here that a 10×10 grid denoted Ω which $\Omega = \bigcup_{p,q=1}^{10} C_{pq}$. At $t = 1$ we assume that the susceptible people are homogeneously distributed with 10.000 in each cell except at the upper right corner cell C_{1010}, where we introduce 50 infectives and 9950 susceptibles and at the lower left corner cell C_{11} where we introduce 500 infectives and keep 9450 susceptibles there, hence the middle of Ω the cell C_{55} we introduce 900 infectives and 9000 susceptibles, with different parameters cited in table 1, we study the case when the epidemic starts from the three cell $\{C_{1010}, C_{55}, C_{11}\}$ i.e three regions (source of infection). The vicinity sets associated with regions or cells C_{11}, C_{55} and C_{1010} are defined by $V_{11} = \{C_{12}, C_{21}, C_{22}\}$, $V_{55} = \{C_{54}, C_{56}, C_{44}, C_{45}, C_{46}, C_{64}, C_{65}, C_{66}\}$ and $V_{1010} = \{C_{109}, C_{99}, C_{910}\}$ respectively. In all of the figures below, the redder part of the colorbars contains larger numbers of individuals while the bluer part contains the smaller numbers.

In order to see the effectiveness of our control strategy, we will consider four cases of the fight against the spread of the disease. In the first case we will restrict ourselves to controlling only the cell in the center, the second situation we control the upper right side, the third case we control the cell at lower left side and finally we combine the three previous cases.

- Case 1: Controlling the center cell
- Case 2: Controlling the upper right cell
- Case 3: Controlling the lower left cell
- Case 4: Combining the three cases.

Case 1 : Controlling the center cell . In this case, C_{55} is considered a source of infection and a quarantine control u_{55} is introduced. After the introduction of quarantine control u_{55} (see

TABLE 1. The description of parameters used for the definition of discrete time systems (4)-(6).

	S_0	I_0	R_0	β	d	γ	Λ_j	α
C_{11}	9450	500	50	0.051	0.16	0.0025	70	0.002
C_{55}	9000	900	100	0.2481	0.1346	0.003	36	0.001
C_{1010}	9950	50	0	0.11	0.219	0.025	80	0.006

its location in the differential system (4) - (6)), it can be deduced from figure 2, which represents the simulations of the functions S, I , R, associated with the case where optimal control approaches the quarantined region becoming geographically isolated from their neighbors. In order to show the importance of the quarantine approach suggested in this article, consider the example of a cell with 8 neighboring cells. As in the previous section, we also examine the results obtained when the disease starts from the three C_{11}, C_{55} and C_{1010} regions. In this way, we can deduce that the control strategy has proved its effectiveness earlier in time. In fact, at instant $i = 100$, most cells, $S^{C_{pq}}$ becomes less important, converges to 8000, however the C_{55} controlled cell becoming geographically isolated from their neighbors, the number of susceptible individuals in the 8 neighboring cells $V_{55} = \{C_{54}, C_{56}, C_{44}, C_{45}, C_{46}, C_{64}, C_{65}, C_{66}\}$ has retained its value of 10000, which is not exactly the same as in the case where there was still no control. Even at times $i = 150$, $i = 200$ the number of susceptible people has decreased more significantly, but luckily we achieve our goal by keeping the number of 8 neighboring cells $V_{55} = \{C_{54}, C_{56}, C_{44}, C_{45}, C_{46}, C_{64}, C_{65}, C_{66}\}$ close to its initial value despite a slight decrease, which is not exactly the same as the case where no control strategy is yet suggested. At time $i = 300$, we can see more clearly that the $S^{C_{55}}$ cell has decreased except for the cells in their neighbors, whereas the $S^{C_{pq}}$ have values between 0, 1000 and 4000 in some cells near the corners. This shows that most of the movements of infected people from the C_{55} have been restricted in recent times. In Fig.2(b) we can deduce that at instant $i = 150$, the numbers $I^{C_{55}}$, $I^{C_{11}}$ and $I^{C_{1010}}$ are at most identical, as shown by the absence of controls. However, the neighboring cells of the C_{55} controlled cell is still not really infected and does not contain any infected individuals. After 200 days, the density of the infected class decreases from 4500 infected when

there was no control to less than 2500 infected in the source of infection when there is optimal control.

We achieve our goal by maintaining the values of the infection that arise nearby set V_{55} close to its initial value in the case of a u_{55} quarantine strategy that concerns the C_{55} cell. At time $i = 300$, we can see more clearly that the $I^{C_{55}}$ cell has grown except for cells in their neighbors, while infection becomes important in cells near corners and borders. This shows that most of the movements of infected people from the C_{55} have been restricted in recent times.

In Fig.2(c) it can be seen that simultaneously, at time $i = 150$, the number$R^{C_{55}}$, $R^{C_{11}}$ and $R^{C_{1010}}$ takes a value close to / equal to 500, while $R^{C_{pq}}$ in the cells of V_{55} is equal to zero and that we are moving away from V_{55}, $R^{C_{pq}}$ is always zero. Similarly, at times $i = 150$, $i = 200$, and $i = 250$ in all C_{pq} cells, the number of people withdrawn increases to 1000 in the corner cells and to 500 in most cells of Ω, and to 1000 when we move forward in time, as we can see it at the moment $i = 300$, while the $R^{C_{55}}$ has not changed significantly.

Case 2 :Controlling the upper right cell . In this case, $C_{10,10}$ is considered a source of infection and a quarantine control $u_{10,10}$ is introduced. After the introduction of the quarantine control $u_{10,10}$ (see its location in the differential system (4) - (6)) figure 3 illustrates shapes of the quarantine control which restrict movements of infected people coming from $C_{10,10}$. In order to show the importance of the quarantine approach suggested in this article, consider the example of a cell with 3 neighboring cells. As in the previous section, we also examine the results obtained when the disease starts from the three (cell) C_{11}, C_{55} and C_{1010} regions. In this way, we can deduce that the control strategy has proved its effectiveness earlier in time. We can see that at instant $i = 100$, the numbers $S^{C_{1010}}$ and $S^{C_{pq}}$ are at most the same as in the case when there was no control strategy. At times $i = 150$, $i = 200$, we can observe that in most of cells $S^{C_{pq}}$ becomes less important, taking values between 0 and 2000 in cells that are close to V_{55} and V_{11}, while in other cells, and as more we move away from V_{55} and V_{11}, it takes values between 2000 and 7000. However, the proximity of controlled cell $C_{10,10}$ ie the 3 neighboring cells $V_{1010} = \{C_{109}, C_{99}, C_{910}\}$ has kept its value of 10000. In fact, even at times $i = 250$ and $i = 300$, $S^{C_{pq}}$ is also the same as before but fortunately again, we reach our goal in keeping number the proximity set $V_{10,10}$ close to its initial value despite some small decrease. Thus, this

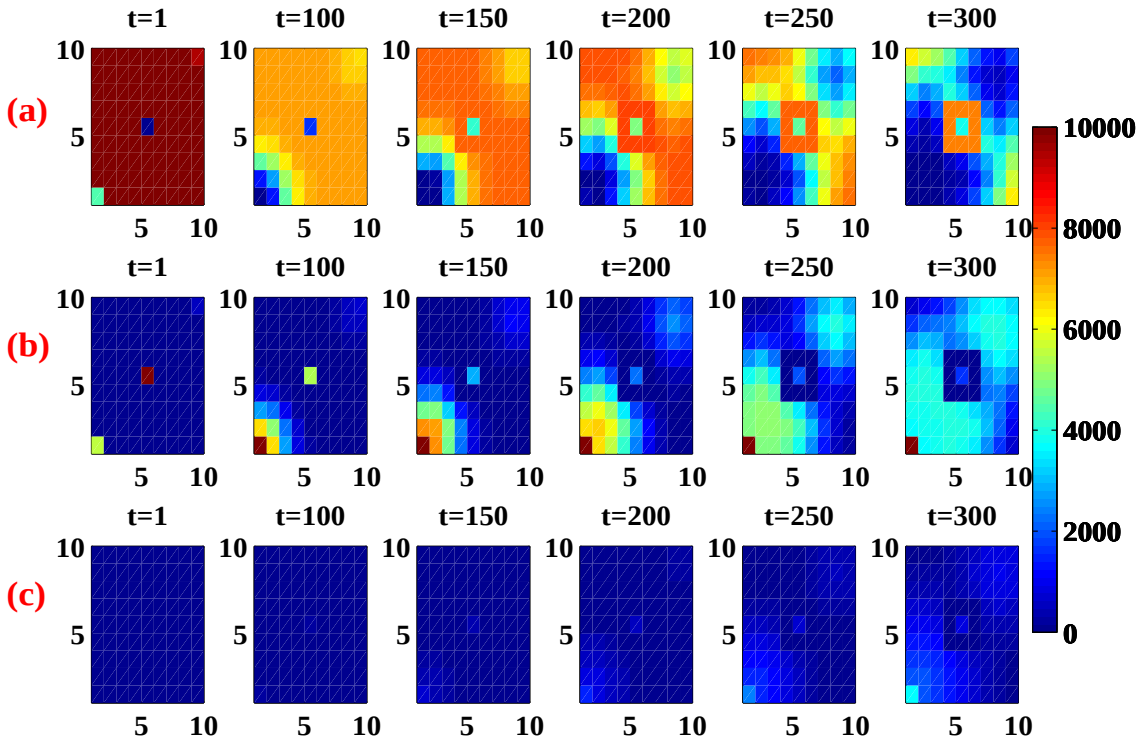

FIGURE 2. States of system (4)–(6) with control u^{55Crs}. (a) Susceptibles behavior with control. (b) Infectives behavior with control. (c) Removed behavior with control

demonstrates that most of movements of infected people coming from the controlled cell C_{1010}, have been restricted in final times.

In Fig. 3(b), we can deduce that at instant $i = 100$, there is an increase in the number of infected cases within most of cells. However, the vicinity of controlled cell $C_{10,10}$ is still not really infected and can not be contains no infected individual. Similarly at times $i = 150$ and $i = 200$, $I^{C_{pq}}$ takes values around 5000 in neighboring cells to V_{55} and V_{11} and about 2000 in other cells except at the 2 opposite corners and borders of Ω. At time $i = 300$, most cells C_{pq} begin to lose some infected individuals due to natural recovery and the number $I^{C_{pq}}$ becomes less and less important at further instants while he vicinity of controlled cell V1010 does not exceed its initial value. In Fig. 3(c) it can be seen that simultaneously, at time $i = 150$, the numbers $R^{C_{11}}$, $R^{C_{55}}$ and $R^{C_{10,10}}$, take a value close to / equal to 500, while $R^{C_{pq}}$, in the vicinity set of $C_{10,10}$ is equal to zero and that we are moving away from $V_{10,10}$, $R^{C_{pq}}$ is always zero. Similarly, at

times $i = 150$, $i = 200$, and $i = 250$ in all C_{pq} cells, the number of people withdrawn increases to 1000 in the corner cells and to 500 in most Ω cells, and to 1000 as we move forward in time, as we can see at time $i = 300$, while the $R^{C_{10,10}}$ has not changed significantly.

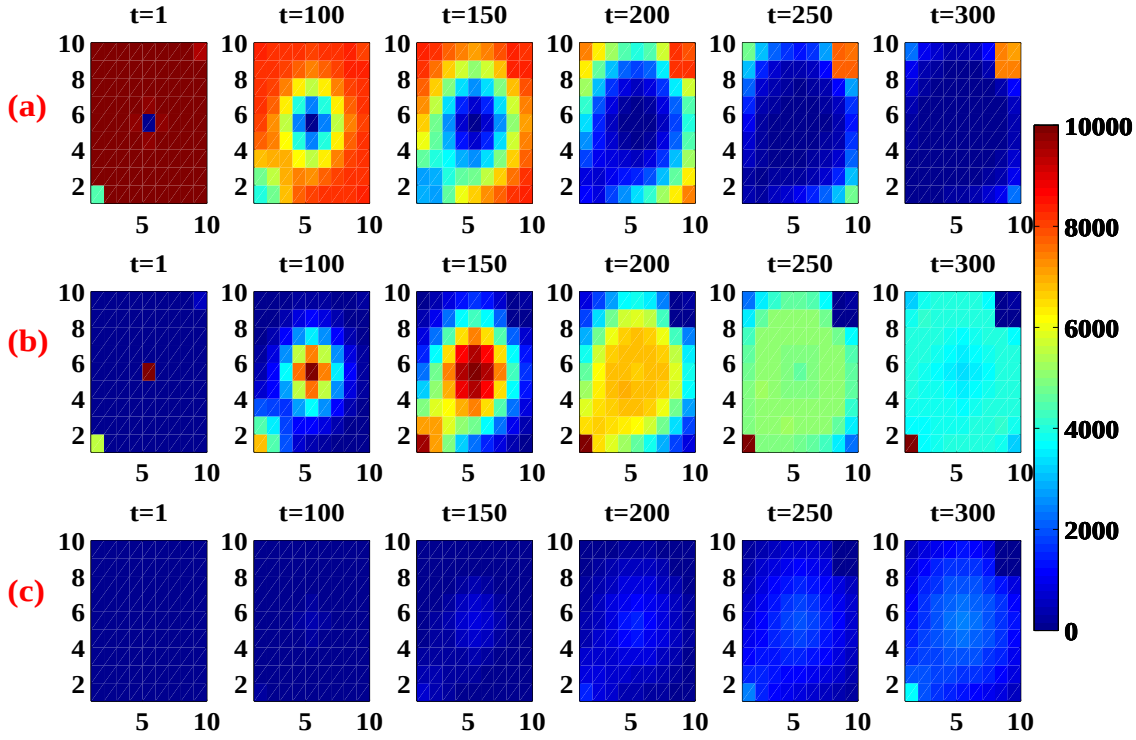

FIGURE 3. States of system (4)–(6) with control $u^{1010Crs}$. (a) Susceptibles behavior with control. (b) Infectives behavior with control. (c) Removed behavior with control

Case 3 : Controlling the lower left cell . In this case, C_{11} is considered a source of infection and a quarantine control u_{11} is introduced. After the introduction of quarantine control u_{11} (see its location in the differential system (4) - (6)). We note that we are interested here, to control a cell with 3 neighboring cells. As shown in figure 4, we can see that the C_{11} controlled cell is becoming geographically isolated from their neighbors. At time $i = 100$ it can be observed that there is a decrease in the number of susceptibles cases within most cells, however the vicinity of the controlled cell V11 does not exceed its initial value. At moments $i = 150$ and $i = 200$, $S^{C_{pq}}$ takes values between 0 and 1000 in neighboring cells which belong toV_{55} and $V_{10,10}$, and

about 4000 in other cells except at the 2 opposite corners and borders of Ω, while the vicinity set of controlled cell V_{11} canned its initial value. at $i = 300$ we can show that the epidemic cover all Ω except the cells in neighboring cells which belong to $V_{11} = \{C_{12}, C_{21}, C_{22}\}$. In Fig.4(b), we can deduce that at instant $i = 150$, there is an increase in the number of infected cells within most cells, however, the vicinity of controlled cell C_{11} is still not really infected and does not contains no infected individual. likewise at moments $i = 150$ and $i = 200$, $I^{C_{pq}}$ takes values around 6000 in neighboring cells and about 4000 in other cells except at the 2 opposite corners and borders of Ω. At time $i = 300$, most cells C_{pq} begin to lose some infected individuals due to natural recovery and the number ICpq becomes less and less important at further instants while he vicinity of controlled cell V11 does not exceed its initial value. In Fig.4(c) it can be seen that simultaneously, at the instant $i = 150$, the numbers $R^{C_{11}}$, $R^{C_{55}}$ and $R^{C_{10,10}}$ take a value close to / equal to 500, while R^{C}_{pq} in the vicinity set of V_{11} is equal to zero and as we move away from V_{11}, $R^{C_{pq}}$ is always zero. Similarly, at times$i = 150$, $i = 200$ and $i = 250$ in all C_{pq} cells the number of people withdrawn increases to 1000 in corner cells and to 500 in most Ω cells and to 1000 when we move forward in time, as we can find it at the instant $i = 300$, while the $R^{C_{11}}$ has not changed significantly.

Case 4 : Combining the three cases. In this case, C_{11}, C_{55} and C_{1010} are considered at source of infection; then, three control variables are introduced representing the quarantine, u_{11}, u_{55} and u_{1010} , in order to block people coming from C_{11}, C_{55} and C_{1010} , respectively. Because the main objective of the whole work is to decrease the number of infected and dead people, by pursuing quarantine control approaches, we deduce by simulations presented in figure 5 that by three controls u_{11}, u_{55} and u_{1010} effect to slow the spread of the infection. Specifically, in Fig.5(b), after 300 days the density of the infected class is decreasing from 4400 infected when there was no control, to less than 2000 infected in the source of infection when there is the optimal control. One of the major benefits of this control is to restrict movements of people coming from regions at high risk of infection from their neighbors and this can be observed in Fig.5(a) where the minimum number of the susceptible people becomes approximately equal to 7407 individuals against less than 100 individuals when there is no controls and that can obviously prove the effectiveness of the quarantine strategy.

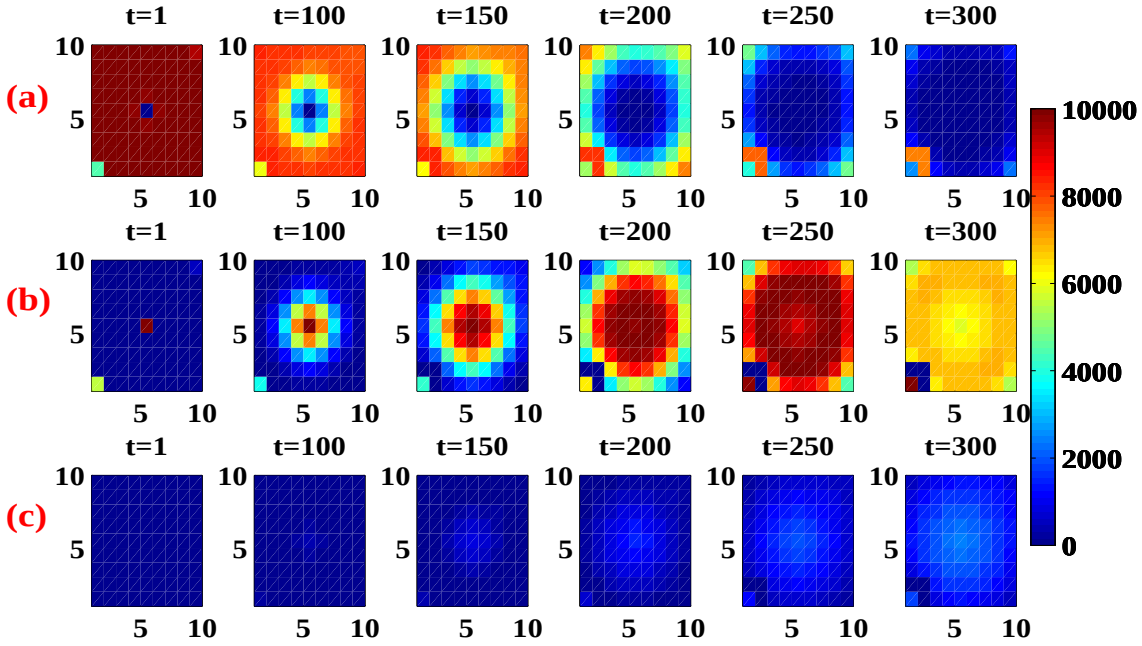

FIGURE 4. States of system (4)–(6) with control u^{11Crs}. (a) Susceptibles behavior with control. (b) Infectives behavior with control. (c) Removed behavior with control

4. CONCLUSION

The main idea of this article is to present an optimal strategy for controlling the spread of an epidemic in a given region, based on a discrete time multi-region epidemic model describing the evolution of the number of susceptible, infected and removed in different regions incorporating the movement of people from one region to another. The regions were assembled into a meshed cell surface where each cell represents a region, to show the impact of an infection that comes from a cell in its vicinity. In fact, by this type of representation, we have succeeded in showing the effectiveness of the neighborhood quarantine control method in isolation of infectious individuals and / or persons known to come into contact with an infectious individual and then we have demonstrated that when we restrict the movements of infected individuals from the target source, we can keep this location safe and without any significant infection.

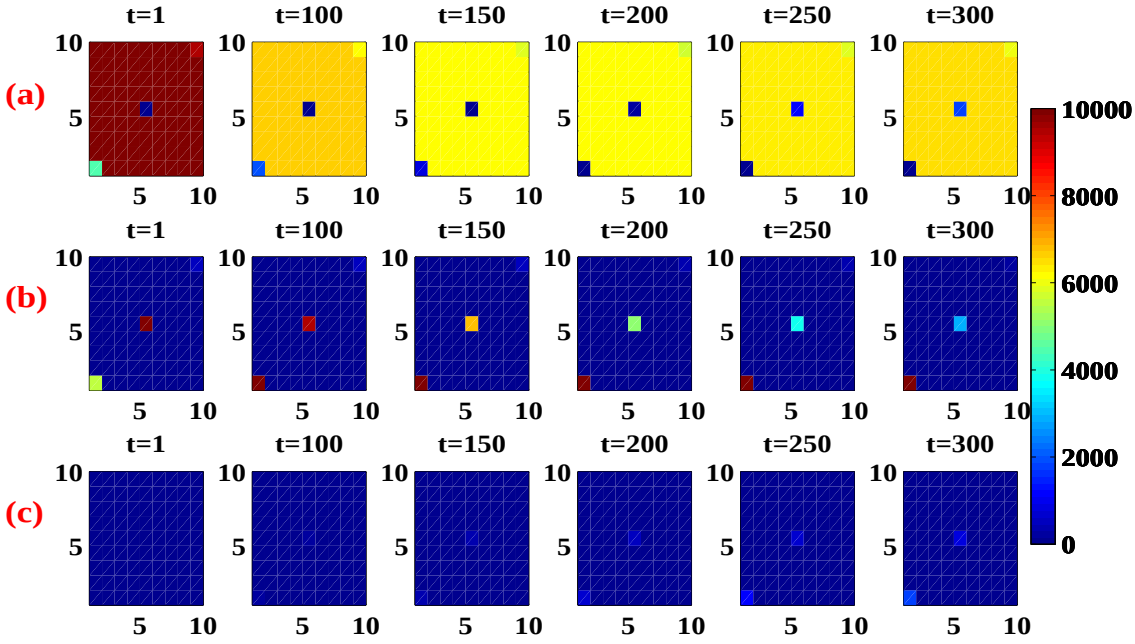

FIGURE 5. States of system (4)–(6) with controls u^{11Crs} , u^{55Crs} and $u^{1010Crs}$.(a) Susceptibles behavior with control. (b) Infectives behavior with control. (c) Removed behavior with control

CONFLICT OF INTERESTS

The author(s) declare that there is no conflict of interests.

REFERENCES

[1] Stöhr, K., A multicentre collaboration to investigate the cause of severe acute respiratory syndrome. Lancet, 361 (9370) (2003), 1730-1733.

[2] World Health Organization Pandemic H1N1 2009 update 78. http://www. who.int/csr/disease/swineflu/en/index.html. Accessed on 11 December 2009.

[3] KOHN, George C. The wordsworth encyclopedia of plague & pestilence. Wordsworth Reference, 1998.

[4] ZINSSER, Hans. Rats, Lice, and History: A Chronicle of Pestilence and Plagues. Black Dog and Leventhal Publishers, New York, 1935.

[5] Arino, J., Davis, J. R., Hartley, D., Jordan, R., Miller, J. M., & Van Den Driessche, P., A multi-species epidemic model with spatial dynamics. Math. Med. Biol. 22 (2) (2005), 129-142.

[6] Okware, S. I., Omaswa, F. G., Zaramba, S., Opio, A., Lutwama, J. J., Kamugisha, J., ... & Lamunu, M., An outbreak of Ebola in Uganda. Trop. Med. Int. Health, 7 (12) (2002), 1068-1075.

[7] Laaroussi, A. E. A., Ghazzali, R., Rachik, M., & Benrhila, S., Modeling the spatiotemporal transmission of ebola disease and optimal control: a regional approach. Int. J. Dyn. Control, 7 (3) (2019), 1110-1124.

[8] PETERSEN, Lyle R. et ROEHRIG, John T. West Nile virus: a reemerging global pathogen. Rev. Bioméd. 12 (3) (2001), 208-216.

[9] Lewnard, J. A., Mbah, M. L. N., Alfaro-Murillo, J. A., Altice, F. L., Bawo, L., Nyenswah, T. G., & Galvani, A. P., Dynamics and control of Ebola virus transmission in Montserrado, Liberia: a mathematical modelling analysis. Lancet Infect. Dis. 14 (12) (2014), 1189-1195.

[10] Camacho, A., Kucharski, A. J., Funk, S., Breman, J., Piot, P., & Edmunds, W. J., Potential for large outbreaks of Ebola virus disease. Epidemics, 9 (2014), 70-78.

[11] Baize, S., Pannetier, D., Oestereich, L., Rieger, T., Koivogui, L., Magassouba, N. F., ... & Tiffany, A., Emergence of Zaire Ebola virus disease in Guinea. New England J. Med. 371 (15) (2014), 1418-1425.

[12] World Health Organ. WHO, Liberian health authorities confirm two cases of Ebola. Reuters. Retrieved March 30, 2014.

[13] Arino, J., Jordan, R., & Van den Driessche, P., Quarantine in a multi-species epidemic model with spatial dynamics. Math. Biosci. 206 (1) (2007), 46-60.

[14] Lee, J., & Jung, E., A spatial–temporal transmission model and early intervention policies of 2009 A/H1N1 influenza in South Korea. J. Theor. Biol. 380 (2015), 60-73.

[15] Ghazzali, R., Laaroussi, A. E. A., Bhih, A. E., & Rachik, M. (2019). On the control of a reaction–diffusion system: a class of SIR distributed parameter systems. Int. J. Dyn. Control, 7 (3) (2019), 1021-1034.

[16] Dabbs, K., Optimal control in discrete pest control models. University of Tennessee Honors Thesis Projects, 2010.

[17] Pontryagin, LS, Boltyanskii, VG, Gamkrelidze, RV, Mishchenko, E., The mathematical theory of optimal processes (International series of monographs in pure and applied mathematics). Interscience, New York, 1962.